https://doi.org/10.5194/hess-2024-209
Preprint. Discussion started: 21 October 2024

Hydrology and Earth System Sciences
Discussions

Towards a Robust Hydrologic Data Assimilation System for Hurricane-induced River Flow Forecasting

[1]Peyman Abbaszadeh, [2]Keyhan Gavahi, [2]Hamid Moradkhani

[1]Department of Civil and Environmental Engineering, Hydrologic Modeling and Assimilation Lab, Portland State University, Portland, OR, USA

[2]Center for Complex Hydrosystems Research, Department of Civil, Construction and Environmental Engineering, The University of Alabama, AL, USA

Correspondence to: Peyman Abbaszadeh (pabbaszadeh@pdx.edu)

https://doi.org/10.5194/hess-2024-209
Preprint. Discussion started: 21 October 2024

Hydrology and Earth System Sciences
Discussions

Abstract

The Hybrid Ensemble and Variational Data Assimilation framework for Environmental Systems (HEAVEN) is a method developed to enhance hydrologic model predictions while accounting for different sources of uncertainties involved in various layers of model simulations. While the effectiveness of this data assimilation in forecasting streamflow have been proven in previous studies, its potential to improve flood forecasting during extreme events remains unexplored. This study aims to demonstrate this potential by employing HEAVEN to assimilate streamflow data from USGS stations into a conceptual hydrologic model to enhance its capability to forecast hurricane-induced floods across multiple locations within three watersheds in the Southeastern United States. The SAC-SMA hydrologic model is driven by two variables: precipitation and Potential Evapotranspiration (PET), collected from phase 2 of the North American Land Data Assimilation System (NLDAS-2) and MODIS (Moderate Resolution Imaging Spectroradiometer) satellite data, respectively. We have validated the probabilistic streamflow predictions during five instances of hurricane-induced flooding across three regions. The results show that this data assimilation approach significantly improves hydrologic model's ability to forecast extreme river flows. By accounting for different sources of uncertainty in model predictions—in particular model structural uncertainty in addition to model parameter uncertainty, and atmospheric forcing data uncertainty, the HEAVEN emerges as a powerful tool for enhancing flood prediction accuracy.

Keywords: Data Assimilation; Hydrologic Modeling; Extreme Event; Hazard; Uncertainty Quantification

https://doi.org/10.5194/hess-2024-209
Preprint. Discussion started: 21 October 2024

Hydrology and Earth System Sciences
Discussions

1. Introduction

Floods rank among the most devastating and destructive natural calamities globally, annually causing significant economic losses and fatalities. The iterature indicates that climate change will amplify the magnitude and frequency of river flooding across the United States (Mallakpour and Villarini, 2015; Alipour et al., 2020b;). This is due to the warming climate that leads to more water evaporating from land and ocean, which in turn increase the size and frequency of the heavy precipitation events, and therefore, escalate the flooding risk (Alipour et al., 2020a; Blöschl et al., 2019). According to the United Nations report, flooding alone affected 2.3 billion people globally from 1995 to 2015 (Wahlstrom and Guha-Sapir, 2015).

A flood modeling system is indispensable to increase the resiliency of communities prone to flooding by minimizing and mitigating their consequences and impacts. Developing an accurate and reliable flood forecasting and inundation system requires multiple components, including: 1) a numerical weather prediction model to estimate the atmospheric forcing variables such as precipitation, 2) a hydrological model to simulate the rainfall-runoff process and other hydrologic fluxes such as streamflow, and 3) a hydrodynamic model for streamflow routing and flood inundation mapping (Grimaldi et al., 2019; Jafarzadegan et al., 2023). Hydrologic and hydrodynamic models together constitute a pivotal part of the flood inundation mapping task, which enables the decision-makers to execute safe urban planning and operational risk management (Annis et al., 2020; Zischg et al., 2018). Existing literature reveals numerous studies concentrating on rainfall-runoff processes and floodplain dynamics, as well as the development of integrated hydrologic and hydrodynamic models. These efforts aim to enhance flood forecasting, assess flood risks, and model flood hazards across spatio-temporal scales (e.g., Felder et al., 2017; Laganier et al., 2014; Mai and De Smedt, 2017; Nguyen et al., 2016; Sindhu and Durga Rao, 2017; Tripathy et al., 2024).

https://doi.org/10.5194/hess-2024-209
Preprint. Discussion started: 21 October 2024

Flood predictions and inundation maps are often inaccurate and erroneous due to different sources of uncertainties involved in different layers of the modeling chain (Ahmadisharaf et al., 2018; Annis et al., 2020; Apel et al., 2004). These include the hydraulic model structure, parameters (e.g., channel and floodplain roughness values), and boundary conditions, that is the upstream and downstream river discharge. While many studies underscore the significance of addressing uncertainties associated with channel and floodplain friction parameters (Aronica et al., 2002; Bates et al., 2004; Papaioannou et al., 2017; Pappenberger et al., 2005; Werner et al., 2005), channel geometry (Bhuyian et al., 2015; Neal et al., 2015), model structure (Dimitriadis et al., 2016; Liu et al., 2019; Petroselli et al., 2019), and input digital elevation model (DEM) resolution (Petroselli et al., 2019) in assessing the uncertainty of inundation mapping, little attention has been given to uncertainties within the hydrologic processes directly impacting flood modeling performance. In most of these studies, the hydrological uncertainties are related to the rating curves (Bermúdez et al., 2017; Di Baldassarre and Montanari, 2009; Domeneghetti et al., 2012; Pappenberger et al., 2006) and the shape of the flow hydrographs (Domeneghetti et al., 2013; Scharffenberg and Kavvas, 2011; Savage et al., 2016), but they did not explicitly account for the uncertainty associated with different components of the hydrologic model predictions, such as the forcing data uncertainty (due to the limitation of measurements and spatiotemporal representativeness of the data), model parameter uncertainty (due to conceptualization of the model and non-uniqueness of parameters), model structural uncertainty due to the imperfect representation of a real system (Pathiraja et al., 2018; Parrish et al., 2012), and initial and boundary condition uncertainty (Abbaszadeh et al., 2018a; Moradkhani et al., 2018a). This study seeks to account for all the aforementioned sources of uncertainties involved in hydrologic model predictions within a Bayesian framework and studies their impacts on hurricane-induced extreme

https://doi.org/10.5194/hess-2024-209
Preprint. Discussion started: 21 October 2024

river discharges across different regions in the Southeastern United States (SEUS). It is expected that reducing hydrologic uncertainties result in improving the accuracy and reliability of flood inundation mapping when the enhanced hydrologic forecasts are utilized to drive the hydrodynamic model.

Bayesian methods have been extensively utilized in a numerous studies to characterize, quantify and reduce the uncertainties in hydrologic model predictions. (Abbaszadeh et al., 2020; Dechant and Moradkhani, 2012; Kuczera and Parent, 1998; Marshall et al., 2004; Moradkhani et al., 2005; Pathiraja et al., 2018b; Yan and Moradkhani, 2016). Data Assimilation (DA) is a well-received Bayesian approach in the hydrometeorological community to account for the uncertainties involved in different layers of hydrologic model predictions by probabilistically conditioning the states of the model on observations (Moradkhani et al., 2005; Liu and Gupta 2007; Clark et al. 2008; Vrugt et al. 2006; Moradkhani et al. 2018; Abbaszadeh et al. 2018). The DA methods based on the Ensemble Kalman Filter (EnKF) and Particle Filter (PF) were designed to recursively estimate both states and parameters. In these methods, Monte Carlo sampling and sequential updating are applied to not only a vector of model parameters but also to a set of prognostic and diagnostic state variables at each assimilation step (see Moradkhani et al., (2018) and references therein). The probability distributions of both model states and parameters are recursively and independently updated at each time step when a new observation becomes available. These approaches provide better state and parameter estimates through which the modeling system enables to evolve consistently over time and consequently result in improved model predictions while accounting for uncertainties (Yan et al. 2015; Plaza et al. 2012; Hain et al. 2012; Lee et al. 2011; Lievens et al. 2016; Dechant and Moradkhani 2012, 2011; Abbaszadeh et al. 2018; Montzka et al. 2013; Koster et al. 2018).

https://doi.org/10.5194/hess-2024-209
Preprint. Discussion started: 21 October 2024

In this study, we utilize a recently developed state-of-the-art hydrologic data assimilation method, hereafter referred to as HEAVEN (Hybrid Ensemble and Variational Data Assimilation framework for Environmental Systems), to address all sources of uncertainties (i.e., forcing data, parameters, model structure, and initial conditions) in hydrologic simulations (Abbszadeh et al., 2019). In particular, we study its usefulness and effectiveness in enhancing peak flow forecasts during an extreme event. The remainder of the paper is organized as follows. In Section 2, we present the materials and methods, encompassing the study areas and datasets, descriptions of the hydrologic model, data assimilation, and calibration methods. Section 3 examines the results of the hydrologic data assimilation and its advantages in enhancing peak flow forecasts. Section 4 outlines the conclusions and provides suggestions for further expanding this research in the future.

2. Materials and Methods

This section first describes study areas and datasets used in this study, then introduces the hydrologic model that is used for streamflow prediction, and provides a summary for the model calibration and data assimilation methods.

2.1 Study Areas

This study is conducted over three watersheds in three different states in the southeast US. Figure 1 illustrates their geographical locations along with all the available USGS stations within those regions. Galveston, Mobile, and Savanah are the three watersheds located in hurricane-prone regions near the coast in the state of Texas, Alabama, and Georgia, respectively. These three watersheds encompass Galveston Bay, Mobile Bay, and Savanah Bay, respectively.

https://doi.org/10.5194/hess-2024-209
Preprint. Discussion started: 21 October 2024

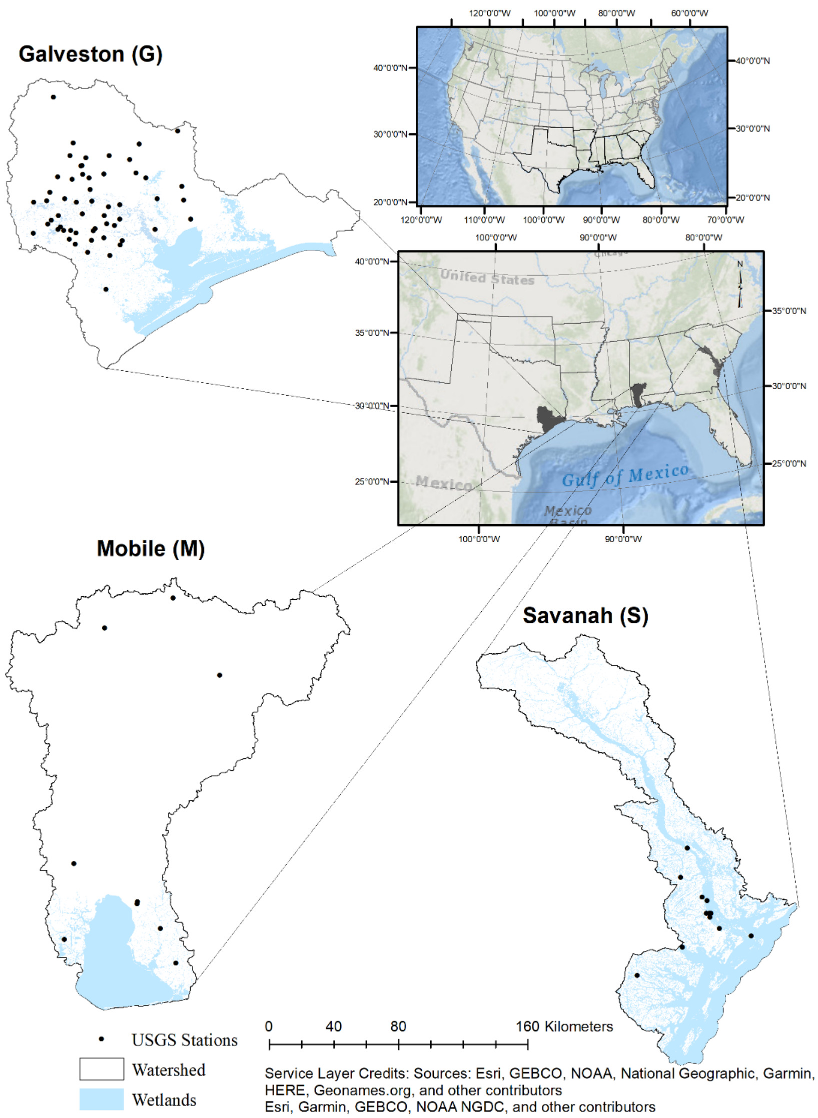

Figure 1. Location of Galveston, Mobile, and Savanah watersheds in three different states in the southeast US. Black points represent the USGS stations operated in each watershed.

To provide a comprehensive analysis and show the robustness of the proposed approach in accounting for the uncertainties involved in hydrologic predictions and its benefit in generating accurate and reliable flood inundated areas, we conducted this study over five hurricane-induced

https://doi.org/10.5194/hess-2024-209
Preprint. Discussion started: 21 October 2024

flooding events in three different regions in the SEUS. These include hurricane Harvey and Rita (in Galveston watershed), Hurricane Ivan (in Mobile watershed), and Hurricane Matthew and Irma (in Savanah watershed). The Galveston watershed comprises nine HUC8s, including 12040202 (East Galveston Bay), 12040203 (North Galveston Bay), 12040102 (Spring), 12040103 (East Fork San Jacinto), 12040201 (Sabine Lake), 12040204 (West Galveston Bay), 12040205 (Austin-Oyster), 12040101 (West Fork San Jacinto), and 12040104 (Buffalo-San Jacinto). The climate in this region is humid subtropical with prevailing winds from the south and southeast that bring heat from the deserts of Mexico and moisture from the Gulf of Mexico. This watershed has a long, hot, and humid summer, such that the temperature exceeds above 32 °C in August, while the winter is often mild and the temperature does not usually drop below 4 °C. Snowfall in Galveston is generally rare, while the rainfall is frequent. With an average of 1000 mm, the rainfall is higher than the national average (767 mm). Hurricanes and tropical storms are notorious for wreaking havoc on the region's economy and environment and putting several communities at risk, including Houston, which is the fifth-largest metropolitan region in the US. In August 2017, hurricane Harvey with heavy rainfall and wind storms hit the Galveston area and caused significant flooding. Many locations around the bay area (i.e., Harris and Galveston counties) experienced more than 760 mm of rain in a few days that resulted in \$23 billion in property damages, according to Reuters report (Ryan McNeill and Duff Wilson, 2017). In September 2005, hurricane Rita swept through east Texas and the Louisiana coast and resulted in extensive flooding, damages, and more than a hundred fatalities. Rita is the most intense tropical cyclone in the history of the Gulf of Mexico. According to the NOAA report (Richard D. Knabb, Daniel P. Brown, 2006), Rita’s wind storm resulted in some flooding across the river networks in northern regions of the Galveston Bay by pushing the river water southward.

https://doi.org/10.5194/hess-2024-209
Preprint. Discussion started: 21 October 2024

Hydrology and Earth System Sciences
Discussions

The Mobile watershed only refers to the lower portion of the Mobile basin which consists of four HUC8s, including 03150204 (lower Alabama), 03160204 (Mobile-Tensaw), 03160205 (Mobile Bay), and 03160203 (Lower Tombigbee). This region is characterized by a warm and temperate climate with well distributed high rainfall throughout the year. Even in the driest month of the year, this area experiences significant rainfall. The precipitation usually is in the form of rain, such that on average the annual rainfall reaches 1600 mm - almost two times more than the US average rainfall per year. In this watershed, summer is long and hot, and the winter is short and cold. In the warmest and coldest months of the year, the temperature usually does not rise above 32 °C and does not fall below 5 °C. In September 2004. Hurricane Ivan made landfall along the coasts from Destin in the Florida panhandle westward to Mobile Bay/Baldwin County, Alabama, according to the NOAA report. The rainfall of this hurricane caused major flooding in both Alabama and northwest Florida. According to the National Weather Services (https://www.weather.gov/mob/ivan), Ivan resulted in nearly $14 billion in damage in both states. The radar-estimated data shows the rainfall associated with hurricane Ivan over the coastline of Alabama (near Orange Beach) reached more than 381 mm and then gradually decreased as the hurricane's eye moved northward.

The third watershed used in this study is Savanah, which is comprised of four HUC8s, including 03060106 (Middle Savannah), 03060109 (Lower Savannah), 03060110 (Calibogue Sound-Wright River), and 03060204 (Ogeechee Coastal). This watershed has a humid subtropical climate with long hot summers and temperate winters. In this region, the precipitation is mainly influenced by the Atlantic Ocean (from the east side) and the Appalachian Mountains (from the west side). The precipitation is usually in the form of rainfall throughout the year with some rare snowstorms that occur in the northern mountainous regions in winter. Climate change has a serious

https://doi.org/10.5194/hess-2024-209
Preprint. Discussion started: 21 October 2024

Hydrology and Earth System Sciences Discussions

impact in Savanah because of the severe heat and intense storms that cause periods of drought and flood, putting the region's water and food supplies at risk. The temperature usually does not go below 4 °C and over 34 °C in the coldest and warmest months of the year. November and August are the driest and wettest months of the year with an average precipitation of 61 mm and 183 mm, respectively. As shown in Figure 1, the predominant land cover in Savanah is wetlands. In October 2016, Hurricane Matthew with strong winds and heavy rainfall hit the coastline of South Carolina and North Carolina and caused extensive coastal and inland flooding. The National Hurricane Center (NHC) reported dozens of deaths and $10 billion in damages across the US East Coast (Stewart, 2017). According to the NOAA report, Hurricane Matthew produced a copious amount of rain that led to record-breaking river levels in some locations in the Savannah region (Liberto, 2016). A year after that, in September 2017, this region was again hit by Category 5 Hurricane Irma. The hurricane's wind speed exceeded 60 mph in the Savanah region that resulted in a significant tidal surge in the Savanah River, according to the National Weather Service. The storm surge and tide together produced maximum inundation levels of 3 to 5 ft above ground level along the coast of Georgia and much of South Carolina that inflicted extensive damages to infrastructure, agriculture, and properties (John P. Cangialosi, Andrew S. Latto, 2017).

2.2 Datasets

We used MODIS (Moderate Resolution Imaging Spectroradiometer) PET (Potential Evapotranspiration), and NLDAS-2 (Phase 2 of the North American Land Data Assimilation System) precipitation forcing data to drive the hydrologic model and estimate the streamflow. The streamflow observations collected from the USGS (United States Geological Survey) stations were used for calibration, assimilation, and validation purposes. To collect the USGS streamflow data, we used *Climata* which is a python package that facilitates acquiring climate and water flow data

https://doi.org/10.5194/hess-2024-209
Preprint. Discussion started: 21 October 2024

from a variety of organizations such as NOAA, NWS (National Weather Service), and USGS. The documentation of this package along with example scripts are available at Earth Data Science (2021).

2.2.1 MODIS

MODIS global evapotranspiration product MOD16 is a gridded land surface ET data set for the global land areas at 8-day, monthly and annual intervals (Mu et al., 2011, 2007). The output variables of the MOD16 product include 8-day, monthly and annual ET, λE (latent heat flux), PET (potential ET), PλE (potential λE), and ET_QC (quality control). In this study, we used MOD16A2 PET product at 500 m spatial resolution and 8-day time-interval. Please note that the pixel values for PET are the sum of all eight days within the composite period. The dataset can be retrieved from https://lpdaac.usgs.gov/products/mod16a2v006/.

2.2.2 NLDAS-2

NLDAS-2 contains quality-controlled, and spatially and temporally consistent meteorological forcing data. Such as surface downward shortwave radiation, surface downward longwave radiation, specific humidity, air temperature, surface pressure, near-surface wind in u and v components, and precipitation rate. In this study, we used precipitation data from the NLDAS_FORA0125_H product, which is a reasonable dataset for operational hydrologic modeling purposes. This dataset is available from 1979 to present with a spatial resolution of 1/8° and temporal resolution of 1 hour (Xia et al., 2012). This data can be retrieved from https://disc.gsfc.nasa.gov/datasets/NLDAS_FORA0125_H_002/summary.

2.3 SAC-SMA Hydrologic Model

In this study, we used Sacramento Soil Moisture Accounting Model (SAC-SMA) to simulate the streamflow at several locations within three different watersheds. The SAC-SMA

(Burnash et al., 1973) is a spatially-lumped continuous soil moisture model that represents each basin vertically by two soil zones: an upper zone and a lower zone. The upper and lower zones represent the short-term storage capacity and long-term groundwater storage, respectively. For descriptions of model parameters and state variables, we refer the readers to our previous study (Abbaszadeh et al., 2018). This model is widely used by the NOAA/NWS for operational flood forecasting in the US (Smith et al., 2003). SAC-SMA produces daily streamflow from daily PET and precipitation data. It is noted that here we disaggregated and aggregated the MODIS PET and NLDAS precipitation data, respectively, to 6-hour interval in order to be consistent with the SAC-SMA hydrologic model that generally runs at a 6-hour time step. SAC-SMA model inputs include 6-hour Mean Areal Precipitation (MAP) and 6-hour Mean Areal Potential Evapotranspiration (MAPE). These variables are calculated by delineating the drainage area contributing to each USGS station for which the hydrologic model is performed.

2.4 Data Assimilation

In this study, we use Hybrid Ensemble and Variational Data Assimilation framework for Environmental Systems, HEAVEN (Abbaszadeh et al., 2019) to account for all sources of uncertainties involved in the hydrologic model simulations. HEAVEN is a data assimilation method built through the combination of a deterministic four-dimensional variational (4DVAR) assimilation method with the particle filter (PF) ensemble data assimilation system. Since we already provided a comprehensive description of this data assimilation approach in the above article, here we briefly describe its formulation and implementation process. HEAVEN provides the possibility that both sequential and variational assimilation approaches can effectively feed each other in a single framework to produce a more complete representation of posterior distributions. The first step is to minimize the weak-constraint 4DVAR cost function (Eq. 1) within

https://doi.org/10.5194/hess-2024-209
Preprint. Discussion started: 21 October 2024

an assimilation cycle and find the optimal initial condition, which is also known as analysis $\mathrm{x_a}$. For the time period of T and assimilation window size K ($[t_0, t_{k=K}]$), the number of assimilation cycles in the HEAVEN becomes $T/_K$. For example, for a one year analysis period of $T = 365$ days, with the assumption of $K = 5$ days, 73 assimilation cycles or windows are defined. In each assimilation cycle, k ranges between 0 to K, where $k = 0$ indicates the initial time step. The optimal solution is the joint maximum likelihood estimate of the state variables within the assimilation window given the observations. The only free variable in the minimization of the cost J is the model state x_0 at the initial time t_0. The optimal solution (analysis) is obtained through an iterative method that, typically, relies on linearized versions of the model and observational operator to obtain a quadratic approximation to the cost J (outer iteration) and adjoint modeling for gradient information.

$$\begin{aligned}
\mathrm{J}(\mathrm{x_0}, \dots, \mathrm{x_K}) &= \mathrm{J^b} + \mathrm{J^o} + \mathrm{J^q} \\
&= \frac{1}{2}\left(\mathrm{x_0} - \mathrm{x_{0,b}}\right)^{\mathrm{T}} \mathrm{B}^{-1}\left(\mathrm{x_0} - \mathrm{x_{0,b}}\right) + \frac{1}{2}\sum_{\mathrm{k}=0}^{\mathrm{K}}\left(\mathrm{y_k} - \mathrm{h_k}(\mathrm{x_k})\right)^{\mathrm{T}} \mathrm{R_k^{-1}}\left(\mathrm{y_k} - \mathrm{h_k}(\mathrm{x_k})\right) \\
&+ \frac{1}{2}\sum_{\mathrm{k}=1}^{\mathrm{K}}\left(\mathrm{x_k} - \mathcal{M}_{\mathrm{k-1}\to\mathrm{k}}(\mathrm{x_{k-1}}, \Theta, \mathrm{u_k})\right)^{\mathrm{T}} \mathrm{Q}^{-1}\left(\mathrm{x_k} - \mathcal{M}_{\mathrm{k-1}\to\mathrm{k}}(\mathrm{x_{k-1}}, \Theta, \mathrm{u_k})\right) \qquad (1)
\end{aligned}$$

k and K show time step in each assimilation window and assimilation window size, respectively. B, $\mathrm{R_k}$, $\mathrm{Q_k}$ specify prior, observation, and model error covariance matrices respectively. Initial deterministic guess for state variables and parameters are also respectively represented by $\mathrm{x_{0,b}}$ and Θ. h and $\mathcal{M}$ represent the observation and model operators. $\mathrm{y_k}$ and $\mathrm{u_k}$ are the observation and forcing data at time step k. To initialize the system, the error covariance matrices are calculated as follows:

$$\mathrm{R_k} = \left(\max\left((\lambda \times \mathrm{y_k}), 1\right)\right)^2 \qquad (2)$$

$$\mathrm{B} = \mathrm{diag}\left((\Omega \times \mathrm{x_{0,b}})^2\right) \qquad (3)$$

https://doi.org/10.5194/hess-2024-209
Preprint. Discussion started: 21 October 2024

$$Q_k = \Gamma \times \mathrm{diag}\left((\pi \times x_{0,b})^2\right) \qquad (4)$$

where λ is the error percentage in observations. Ω represents the error percentage in initial state variables $x_{0,b}$. π is the error percentage in model structure and Γ is the model error covariance inflation ($\Gamma \geq 1$) or deflation factor ($\Gamma \leq 1$). Since here the model covariance error is assumed to be static and does not vary in time, therefore in equation 1, Q_k becomes Q. The initial guess for the model parameters is obtained using the Latin Hypercube Sampling (LHS) approach. Since the minimum and maximum values of the model parameters are predefined (Abbaszadeh et al., 2018), the ensemble members of model parameters θ^i can be generated using the LHS. Here, the 4DVAR cost function is executed in a deterministic way, therefore it requires an ensemble mean of θ^i, which is calculated using the equation (5). N is the ensemble size.

$$\Theta = \frac{1}{N}\sum_{i=1}^{N}\theta^i \qquad (5)$$

The linearization of observation h and model $\mathcal{M}$ operations is required for performing variational data assimilation approaches. This hinders their use in hydrological applications because such linearizations are not usually feasible. To address this problem, we minimize the 4DVAR cost function and find the optimal solution x_a using the Nelder-Mead algorithm (Nelder and Mead, 1965), which is a derivative-free optimization method. 4DVAR seeks the initial condition such that the forecast best fits the observations within the assimilation interval. We specify the model parameters Θ at each time step within the assimilation interval. We then find the best initial state variables (also known as analysis) x_a by minimizing the 4DVAR cost function.

Up to this point, the optimal initial condition x_a within the first assimilation window is obtained. To perform the particle filtering DA within the same assimilation window, we use x_a as an initial guess (prior information) with some error that follows a Gaussian distribution. In

https://doi.org/10.5194/hess-2024-209
Preprint. Discussion started: 21 October 2024

equation (6), $\mathrm{x}_0^{\mathrm{i}}$ is the initial state ensemble members and B is the prior error covariance matrix used in the 4DVAR cost function.

$$\mathrm{x}_0^{\mathrm{i}} = \mathrm{x}_{\mathrm{a}} + \varepsilon^{\mathrm{i}} \qquad \varepsilon^{\mathrm{i}} \sim \mathrm{N}(0, \mathrm{B}) \qquad (6)$$

To ensure that an appropriate initial condition x_0^i is replicated for cycle τ, which later leads to better estimation of the posterior distributions in that window interval, we run the forward model for cycle τ using two initial ensemble scenarios: (1) x_0^i and (2) state posterior distribution obtained in the last time step ($k = K$) of assimilation cycle $\tau - 1$ (x_K^i). Under these two initial conditions, we calculate y_k^i for ensemble members within the assimilation interval $[t_0, t_K]$, and based on their discrepancies from the observations Obs_k, one can decide to preserve the particles x_0^i or replace them with those already available from the previous cycle $\tau - 1$.

Here, we describe the implementation of the Evolutionary Particle Filter with Markov chain (EPFM) data assimilation approach (Abbaszadeh et al., 2018). EPFM is a sequential data assimilation technique based on the combination of particle filtering, MCMC (Markov chain Monte Carlo), and GA (Genetic Algorithm). EPFM is performed within the assimilation window for which the initial condition was obtained from the 4DVAR approach. Her,e we provide a brief overview of the EPFM algorithm and for more information, we refer the readers to the original article (Abbaszadeh et al., 2018).

Equations 7 and 8 describe the generic nonlinear dynamic system, where $\mathrm{x}_{\mathrm{t}} \in \mathbb{R}^{\mathrm{n}}$ and $\theta \in \mathbb{R}^{\mathrm{d}}$ are vectors of uncertain state variables and model parameters, respectively. u_t represents the uncertain forcing data, $\mathrm{y}_{\mathrm{t}} \in \mathbb{R}^{\mathrm{m}}$ indicates a vector of observation data, ω_{t} and υ_{t} are the model and measurement errors, respectively, which are assumed to be independent and follow white noises with mean zero and covariance Q_{t} and R_{t}.

https://doi.org/10.5194/hess-2024-209
Preprint. Discussion started: 21 October 2024

Hydrology and Earth System Sciences
Open Access
Discussions

$$x_t = \mathcal{M}(x_{t-1}, u_t, \theta) + \omega_t \qquad \omega_t \sim N(0, Q_t) \qquad (7)$$

$$y_t = h(x_t) + \upsilon_t \qquad \upsilon_t \sim N(0, R_t) \qquad (8)$$

The following formula is used to calculate the posterior distribution of the state variables at time t.

$$p(x_t|y_{1:t}) = p(x_t|y_{1:t-1}, y_t) = \frac{p(y_t|x_t)p(x_t|y_{1:t-1})}{p(y_t|y_{1:t-1})} = \frac{p(y_t|x_t)p(x_t|y_{1:t-1})}{\int p(y_t|x_t)p(x_t|y_{1:t-1})dx_t} \qquad (9)$$

$$p(x_t|y_{1:t-1}) = \int p(x_t, x_{t-1}|y_{1:t-1})dx_{t-1} = \int p(x_t|x_{t-1})p(x_{t-1}|y_{1:t-1})dx_{t-1} \qquad (10)$$

where $p(y_t|x_t)$ is the likelihood at time step t, $p(x_t|y_{1:\,t-1})$ is the prior distribution, and $p(y_t|y_{1:t-1})$ is the normalization factor. The marginal likelihood function $p(y_{1:\,t})$ and the normalization factor $p(y_t|y_{1:\,t-1})$ can be calculated using equations 11 and 12, respectively.

$$p(y_{1:t}) = p(y_1)\prod p(y_t|y_{1:t-1}) \qquad (11)$$

$$p(y_t|y_{1:t-1}) = \int p(y_t, x_t|y_{1:t-1})dx_t = \int p(y_t|x_t)p(x_t|y_{1:t-1})dx_t \qquad (12)$$

In hydrologic data assimilation based on particle filtering, the posterior distribution is approximated using a set of particles with associated weights.

$$p(x_t|y_{1:t}) \approx \sum_{i=1}^{N} w^{i+}\delta(x_t - x_t^i) \qquad (13)$$

where w^{i+}, δ and N denote the posterior weight of the i-th particle, Dirac delta function, and the ensemble size, respectively. The posterior weight is normalized as follows:

$$w^{i+} = \frac{w^{i-}.\,p(y_t|x_t^i, \theta_t^i)}{\sum_{i=1}^{N} w^{i-}.\,p(y_t|x_t^i, \theta_t^i)} \qquad (14)$$

https://doi.org/10.5194/hess-2024-209
Preprint. Discussion started: 21 October 2024

Hydrology and Earth System Sciences
Open Access
Discussions

where w^{i-} is the prior particle weights, and the $p(y_t|x_t^i, \theta_t^i)$ can be computed from the likelihood $L(y_t|x_t^i, \theta_t^i)$. To calculate this, for simplicity, a Gaussian likelihood is used as follows:

$$L(y_t|x_t^i, \theta_t^i) = \frac{1}{\sqrt{(2\pi)^m |R_t|}} \exp\left[-\frac{1}{2}\left(y_t - h(x_t^i)\right)^T R_t^{-1} \left(y_t - h(x_t^i)\right)\right] \qquad (15)$$

Within this data assimilation method, GA evolutionary cycle is used to shuffle the particles. The particles' weights (w^{i+}) are considered as the fitness value. The particles (population) are sorted in descending order of their fitness values to perform the roulette wheel selection method and select the parent particles for crossover operation and generate offsprings (new particles). Crossover probability refers to a portion of particles that is used for crossover operation. To further increase the diversity of the offspring particles, a mutation operator with a probability is executed. For more information about the crossover and mutation operators and their equations, we refer the readers to Abbaszadeh et al. (2018). The MCMC approach is used to either accept or reject the new offspring particles (proposal state variables). This process requires re-running the model from $t-1$ to t using x_{t-1}^i (state variables before using GA operators) and $x_{t-1}^{i,p}$ (state variables after using GA operators). To accept or reject the proposal states, the metropolis acceptance ratio α is calculated using equation 16.

$$\alpha = \min\left(1, \frac{p(x_t^{i,p}, \theta_t^{i-}|y_{1:t})}{p(x_t^{i-}, \theta_t^{i-}|y_{1:t})}\right) = \min\left(1, \frac{p(y_{1:t}|x_t^{i,p}, \theta_t^{i-}).\, p(x_t^{i,p}|\theta_t^{i-}, y_{1:t-1})}{p(y_{1:t}|x_t^{i-}, \theta_t^{i-}).\, p(x_t^{i-}|\theta_t^{i-}, y_{1:t-1})}\right) \qquad (16)$$

where $p(x_t^{i,p}, \theta_t^{i-}|y_{1:t})$ is the proposed joint probability distribution.

$$p(x_t^{i,p}, \theta_t^{i-}|y_{1:t}) \propto p(y_t|x_t^{i,p}, \theta_t^{i-}).\, p(x_t^{i,p}|\theta_t^{i-}, y_{1:t-1}).\, p(\theta_t^{i-}|y_{1:t-1}) \qquad (17)$$

$$x_t^{i,p} = \mathcal{M}(x_{t-1}^{i,p}, u_t^i, \theta_t^{i-}) \qquad (18)$$

https://doi.org/10.5194/hess-2024-209
Preprint. Discussion started: 21 October 2024

where $p\left(y_t \middle| x_t^{i,p}, \theta_t^{i-}\right)$ is computed using equation 15 and the proposal state Probability Density Function (PDF) $p\left(x_t^{i,p} \middle| \theta_t^{i-}, y_{1:t-1}\right)$ is calculated with the assumption that it follows the marginal Gaussian distributions with mean μ_t (Eq. 20) and variance σ_t^2 (Eq. 21). To calculate the proposal PDF, the weighted mean and variance of the Gaussian distribution are calculated as follows:

$$x_t^{i-} = \mathcal{M}\left(x_{t-1}^{i+}, u_t^i, \theta_t^{i-}\right) \qquad (19)$$

$$\mu_t = \sum w_{t-1}^{i+} x_t^{i-} \qquad (20)$$

$$\sigma_t^2 = \sum w_{t-1}^{i+} \left(x_t^{i-} - \mu_t\right)^2 \qquad (21)$$

Using the accepted proposal state variables, the posterior weights are recalculated using equation 14 and used to compute effective sample size. The resampling step within the sequential data assimilation approach has been already explained in our previous article (Moradkhani et al., 2012), we refer the readers to this publication for more information. Here, we explain how and what information we collect during the sequential filtering process to update the prior (background) error covariance matrix B, which is used in the next assimilation cycle within the 4DVAR cost function. Using equation 22, the best estimates of the model state variables and parameters are acquired as the expected values of their posterior distributions at each time step within the assimilation window.

$$\bar{x}_k^+ = \frac{1}{N}\sum_{i=1}^{N} x_k^{i+} \quad \text{and} \quad \bar{\theta}_k^+ = \frac{1}{N}\sum_{i=1}^{N} \theta_k^{i+} \qquad \forall k = 1, \ \ldots, \ K \qquad (22)$$

$$\eta_k = \bar{x}_k^+ - \mathcal{M}_{k-1\to k}(\bar{x}_{k-1}^+, \bar{\theta}_k^+, u_k) \qquad (23)$$

$$q = \frac{1}{K}\sum_{k=1}^{K} \eta_k \qquad (24)$$

https://doi.org/10.5194/hess-2024-209
Preprint. Discussion started: 21 October 2024

Hydrology and Earth System Sciences
Open Access
Discussions

$$\mathrm{B_d} = \frac{1}{\mathrm{K}-1}\sum_{\mathrm{k}=1}^{\mathrm{K}}[\eta_{\mathrm{k}} - \mathrm{q}][\eta_{\mathrm{k}} - \mathrm{q}]^{\mathrm{T}} \tag{25}$$

$$\mathrm{B_s} = \mathrm{B} \tag{26}$$

$$\mathrm{B} = (\gamma \times \mathrm{B_s}) + (1-\gamma) \times \mathrm{B_d} \qquad 0 \le \gamma \le 1 \tag{27}$$

η_k and q represent the estimate of model error and model error bias at each time within the assimilation window. In this approach, we operate the EPFM filter within the assimilation window for which the best initial condition is estimated by 4DVAR method. In doing so, the question arises as how to use the deterministic (single) initial condition achieved by 4DVAR method to initialize the EPFM filter, which is an ensemble-based approach. To cope with this problem, we define a prior error covariance B, which involves two components: dynamic (B_d) and static (B_s) prior error covariances, to perturb the deterministic solution of 4DVAR approach and generate best initial condition for the EPFM filter. $\mathrm{B_d}$ is the dynamic prior error covariance matrix in the assimilation cycle introduced by Shaw and Daescu (2016). B is the prior error covariance matrix from the previous assimilation cycle. $\mathrm{B_s}$ is the static prior error covariance matrix at the current assimilation cycle. The prior error covariance matrix B is updated using equation 27. γ is a tuning factor, which determines the contribution of model error within the current assimilation cycle. To facilitate the reproduction of HEAVEN, Figure 2 presents a schematic summarizing all the processes involved within this approach.

https://doi.org/10.5194/hess-2024-209
Preprint. Discussion started: 21 October 2024

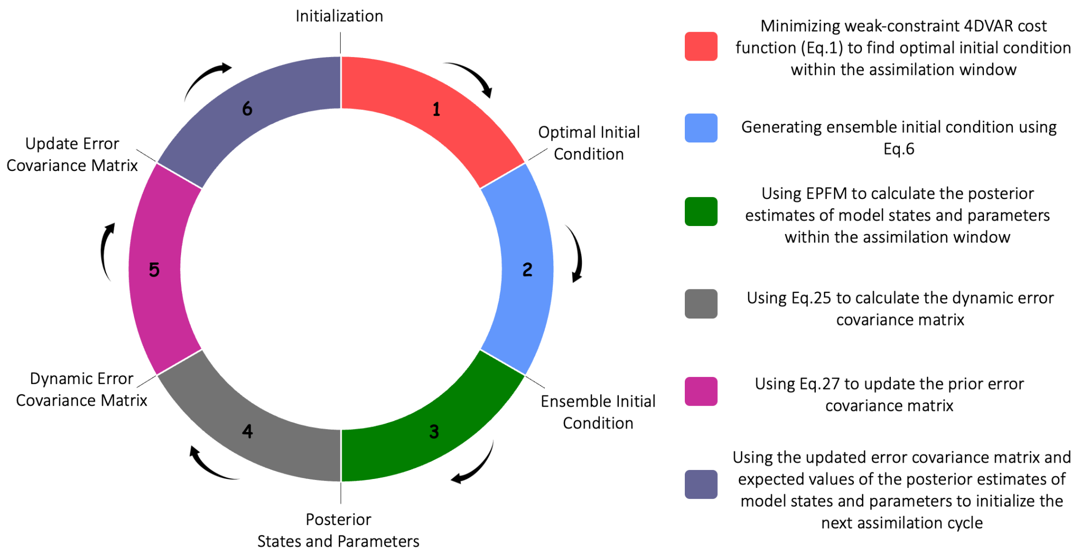

Figure 2: A schematic summarizing all the processes in HEAVEN.

2.5 Model Calibration and Validation

Figure 3 illustrates the model calibration and validation periods used for all three watersheds. As depicted in the figure, the validation period was chosen to encompass the time frame of extreme flooding events in all study regions. This ensures the applicability of the calibrated model for predicting future events. In this study, we employ the SAC-SMA model to simulate flooding events triggered by hurricanes occurring post-2001, as the MODIS-derived PET data necessary to drive the hydrologic model is available starting from 2001. Recent studies (Bennett et al., 2019; Bowman et al., 2017) showed that using MODIS PET as input to the SAC-SMA model results in more reliable streamflow simulations compared to traditional evapotranspiration (ET) demand. For the hydrologic model calibration, we used the Shuffled Complex Evolution (SCE-UA) optimization technique introduced by Duan et al. (1992). In this study, we do not provide a detailed explanation of the SCE-UA method; instead, we refer the readers to the original articles for further information (Duan et al., 1992, 1993). We calibrated 14

Hydrology and Earth System Sciences
Open Access
Discussions

parameters within the SAC-SMA model using 10-years historical USGS streamflow observations, consistent with the calibration period suggested by the NOAA/National Weather Service (Smith et al., 2003). The optimal parameter values at each USGS station were found by maximizing Nash Sutcliffe Efficiency (NSE) objective function that simultaneously considers mean, low, and high flows (Samuel et al., 2011).

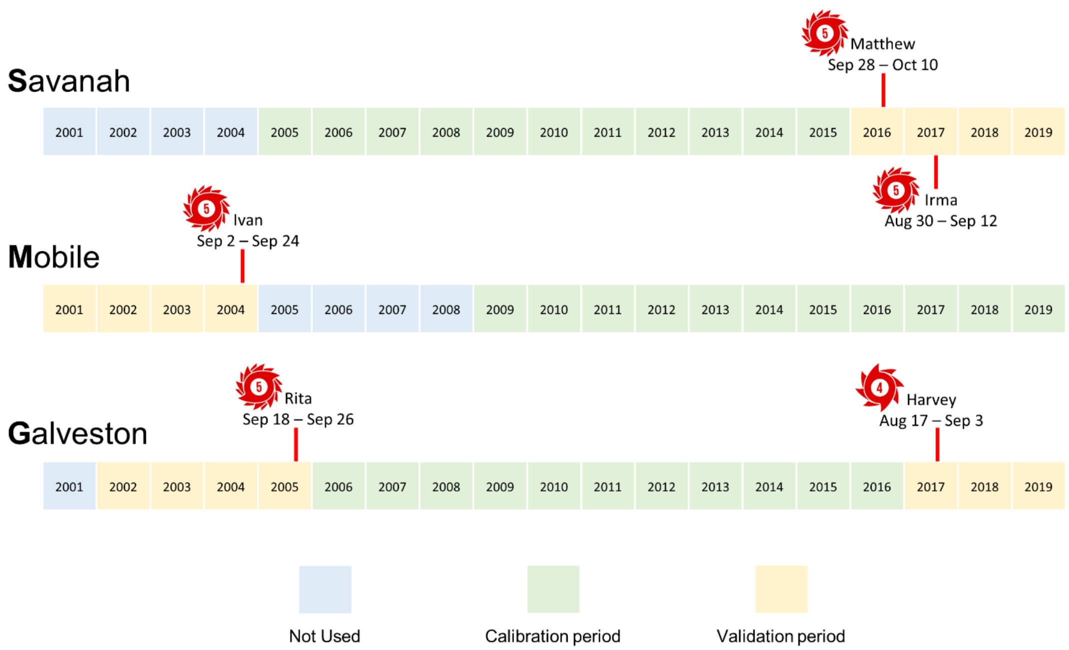

Figure 3. The calibration and validation periods considered in this study for three watersheds, along with the hurricane events and their respective durations.

3. Results and Discussions

This study aims to account for all sources of uncertainties involved in hydrologic model predictions and their impact on improving hurricane-induced extreme river discharges across different regions in the SEUS. This section summarizes the performance of the SAC-SMA hydrologic model during both the calibration and validation periods. It then explains the data assimilation settings along with the streamflow simulation capability of the SAC-SMA model with

https://doi.org/10.5194/hess-2024-209
Preprint. Discussion started: 21 October 2024

Hydrology and Earth System Sciences
Open Access
Discussions

and without data assimilation. The study is conducted in multiple locations across three watersheds in the southeastern US during hurricane events**.**

3.1 SAC-SMA Model Calibration and Validation

Figure 4 illustrates the performance of the SAC-SMA model during both the calibration and validation periods across all study regions utilized in this research. As previously mentioned, for parameter calibration of the SAC-SMA model, we utilized ten years of historical USGS streamflow observation data, while model validation was conducted over a four-year period encompassing flooding from various hurricane events (as shown in Figure 3). Within this figure, the correlation coefficient (R), bias, and root mean square error (RMSE) represent the statistical measures of the relationship between simulated and observed streamflow values. We remind that in this study, we run the hydrologic model over those USGS locations that have not been affected by the backwater effect of the downstream flow and the streamflow observations have always been positive. These USGS locations are shown in Figure 1 with black dots. The results confirm that although the SAC-SMA model was calibrated over the periods for which the river networks within the watersheds have not experienced flow as much as the validation periods, the model parameters were properly calibrated to simulate the streamflow. The temporal resolution of streamflow simulation is hourly, aligning with the requirements for flash flood inundation mapping and forecasting. However, data assimilation occurs at a daily time scale to match the output frequency of the SAC-SMA model. This strategy aims to minimize the impact of instantaneous streamflow changes on parameter updates during the assimilation process. While assimilating streamflow at sub-daily intervals could be advantageous for adjusting model state variables such as soil moisture storage, it is not anticipated to significantly contribute to updating model parameters, which typically vary at coarser time scales.

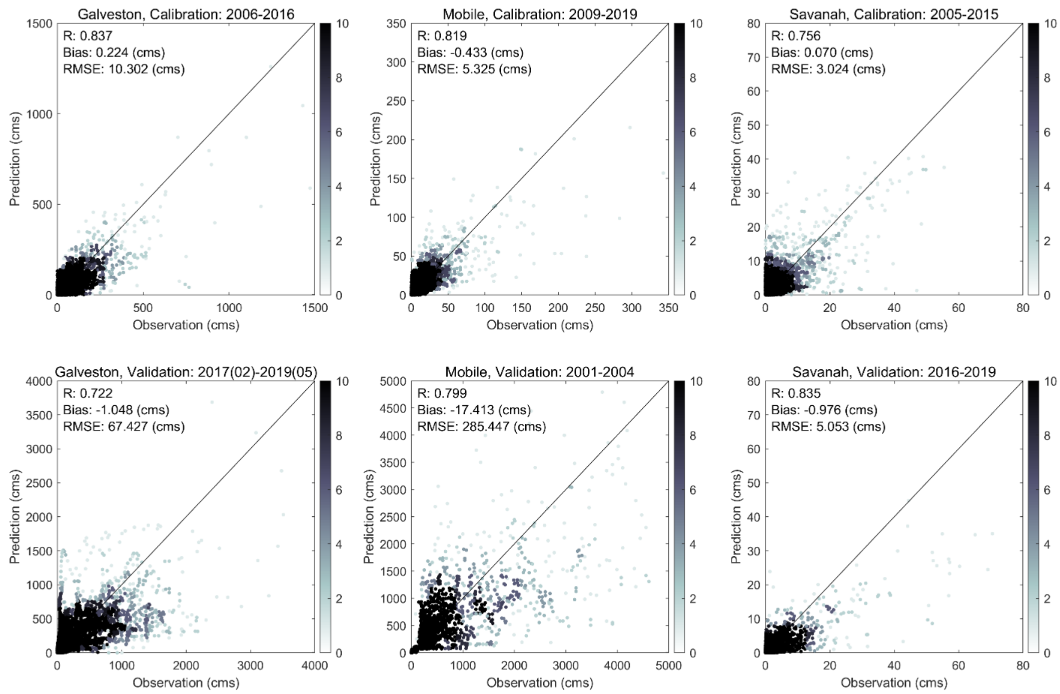

Figure 4. The performance of the SAC-SMA model during the calibration and validation periods over three watersheds in the southeast US.

Figure 5 illustrates the model performance (i.e., correlation coefficient and RMSE) across the USGS stations within the Galveston watershed. Figure S1 in the supplementary file shows the same results for the other two watersheds, Mobile and Savanah. The results for the Galveston watershed show that the calibrated SAC-SMA model accurately simulates the streamflow across almost the entire region except the two USGS stations located downstream of the Lake Livingston Dam. The primary function of this dam is flood control. Further analysis revealed that the lower performance of the model at these locations is attributed to the heavy rainfall of Hurricane Harvey that forced the Trinity River authority to release a record 110,600 ft^3/s from Lake Livingston Dam (The Seattle Times, 2021), which resulted in significantly increasing the river flow. A similar event happened in the case of Hurricane Rita that led to the significant flow increase in the Trinity River

https://doi.org/10.5194/hess-2024-209
Preprint. Discussion started: 21 October 2024

and severe flooding (TPWD, 2021). Although the SAC-SMA hydrologic model successfully simulated river flow across all the USGS stations within the Galveston watershed, it could not provide reliable streamflow simulation along the Trinity River due to the water release from Lake Livingston Dam during the Hurricanes Rita and Harvey. For the Mobile watershed, as shown in Figure S1 in the supplementary file, there is a good agreement between the simulated and observed river discharge values across all USGS stations except station #02428400. Further investigations revealed that the river discharge at this location is computed based on flow through the Claiborne Dam (for more information, please see USGS, 2021b). During Hurricane Ivan, the flow at this USGS station reached more than 2800 m^3/s probably due to water release from the Claiborne Dam that consequently resulted in higher downstream river discharge.

https://doi.org/10.5194/hess-2024-209
Preprint. Discussion started: 21 October 2024

Hydrology and Earth System Sciences
Discussions

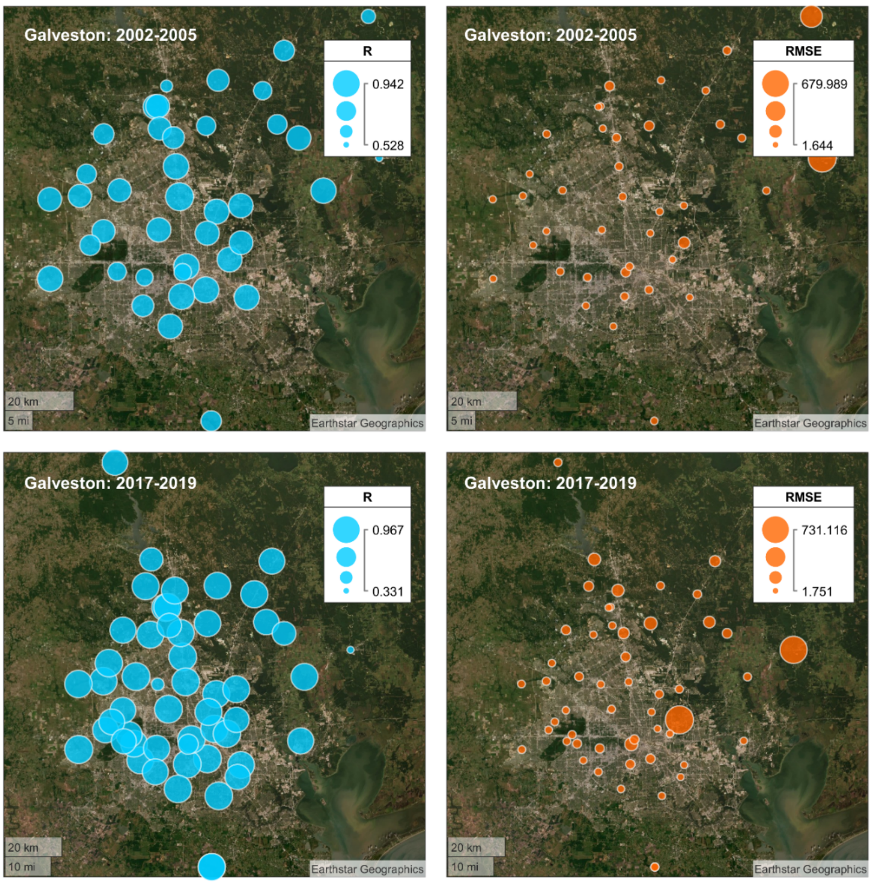

Figure 5. SAC-SMA model performance over the validation period across the USGS stations within the Galveston watershed.

3.2 Improving Streamflow Forecasting using Data Assimilation

The primary goal of this research is to employ a data assimilation technique to account for all sources of uncertainty in SAC-SMA model simulation and provide a more accurate and reliable streamflow prediction. The data assimilation approach used in this study was developed recently by the authors of this study and is used here for the first time to predict streamflow values during multiple hurricane events with heavy rainfall across different locations in the Southeast US. As previously stated, the primary objective of our study is to assess the degree to which the developed

https://doi.org/10.5194/hess-2024-209
Preprint. Discussion started: 21 October 2024

Hydrology and Earth System Sciences
Discussions

data assimilation technique improves the prediction of extreme river flow caused by hurricanes. This section summarizes the performance of the SAC-SMA model after using the data assimilation. The meteorological forcing data including precipitation and PET are assumed to have log-normal and normal error distributions with a relative error of 25% in the DA setting (DeChant and Moradkhani, 2012). This assumption ensures that the meteorological observations' errors due to spatial heterogeneity inherent in these variables and sensor errors are accounted for. The model error is assumed to follow a normal distribution with a relative error of 25%. Unlike the other data assimilation techniques, HEAVEN enables characterizing, quantifying, and taking into account the model structural uncertainty using an explicit form of model error covariance matrix within the data assimilation process. This feature of our developed data assimilation method is specifically more important in this study as we simulate the peak streamflow during hurricane events. As we discussed in our previous paper (Abbaszadeh et al., 2019), in this data assimilation technique, the background error covariance matrix B gets adaptively inflated when the model attempts to simulate extreme values. This error covariance matrix inflation not only helps the 4DVAR objective function to find the optimal initial condition within the assimilation window (Cheng et al., 2019; Liu et al., 2008; Trémolet, 2007), but also ensures exploring the larger feasible solution space when the model states are being corrected within the particle filtering process, which results in a more complete representation of posterior distributions.

Here, we report the performance measures (i.e., correlation coefficient and RMSE) based on an ensemble size of 100 for one-day ahead streamflow forecasting. Figures S2 and S3 show the model performance after using data assimilation across all USGS stations located within the study regions. It should be noted that these results are based on an ensemble size of 100, but of course, larger ensemble sizes would have resulted in better posterior estimates and more accurate and

https://doi.org/10.5194/hess-2024-209
Preprint. Discussion started: 21 October 2024

Hydrology and Earth System Sciences
Discussions

reliable streamflow forecasts. We realized that while data assimilation improved the SAC-SMA model performance across the majority of stations, in some locations the results remained suboptimal. Further investigation revealed that these are the same locations previously identified as being heavily influenced by upstream dam water release during hurricane events. These locations can not be used as upstream boundary conditions for hydrodynamic modeling (which is part of our future study) as they are heavily influenced by water release policy during the hurricane events that altered the natural flow of the river, where hydrologic models most often fail to perform. Given that the ensemble streamflow forecasts produced in this study are commonly utilized to drive hydrodynamic models for flood inundation forecasting and mapping, our focus is specifically directed towards assessing the impact of data assimilation on improving streamflow forecasts during peak flow conditions resulting from hurricane events. Figure 6 depicts how data assimilation improved streamflow forecasting during peak flow conditions across USGS stations in the Galveston watershed during Hurricane Harvey. A similar analysis is also shown in Figure 7 for other watersheds and hurricane events, including Galveston-Rita, Mobile-Ivan, Savanah-Matthew, and Savanah-Irma. The findings revealed that, while data assimilation improved the SAC-SMA streamflow forecasting skill almost across the entire USGS station networks on the peak flow day of Hurricane Harvey, its contribution to improving streamflow forecasting in Hurricane Rita is marginal. Unlike Hurricane Harvey where streamflow reached a peak gradually over the course of a few days (USGS, 2021a), in the case of Hurricane Rita, the streamflow jumped from less than 28 m^3/s (September 23) to more than 566 m^3/s (September 24) in a single day (according to station # 08066500 Trinity Rv at Romayor, TX), such that the hydrologic model failed to detect the unexpected high flow on September 24 despite accurate initialization on September 23 (USGS, 2021b).

https://doi.org/10.5194/hess-2024-209
Preprint. Discussion started: 21 October 2024

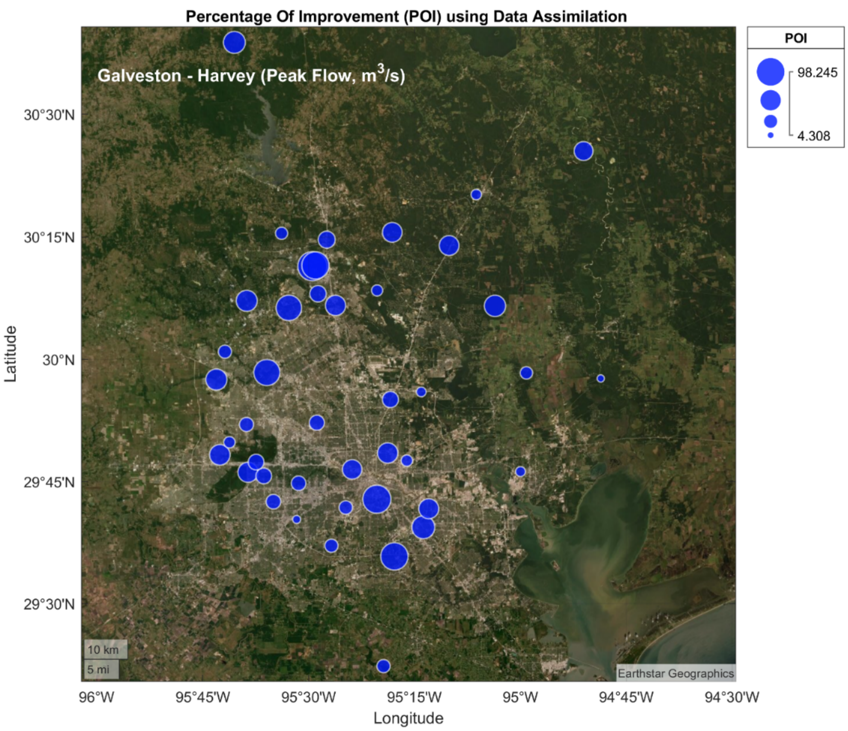

Figure 6. Streamflow forecast improved by data assimilation during peak flow conditions across the USGS stations within the Galveston watershed.

For Hurricanes Ivan and Matthew in Mobile and Savanah, the percentage of improvement in SAC-SMA model peak flow forecasts with data assimilation ranged from 21% to 46% and 5% to 46%, respectively, depending on the location of USGS stations. Understanding and explicitly quantifying the degree to which each source of uncertainties, i.e., meteorological forcing, model parameters, initial condition, model structure, and parametrization, affects the final hydrologic model outputs is not feasible as they all are connected and collectively contribute to degrading model performance. Our developed data assimilation technique, HEAVEN, has an explicit form of covariance error matrix for each source of uncertainty that feeds each other during the assimilation process representing the interaction between different sources of uncertainties

https://doi.org/10.5194/hess-2024-209
Preprint. Discussion started: 21 October 2024

involved in different layers of model simulations. This results in a better representation of posterior distribution and reduction of uncertainty in hydrologic modeling. Due to this reason, we see that the data assimilation approach used in this study is an effective technique to improve the streamflow forecasting skill during hurricane events.

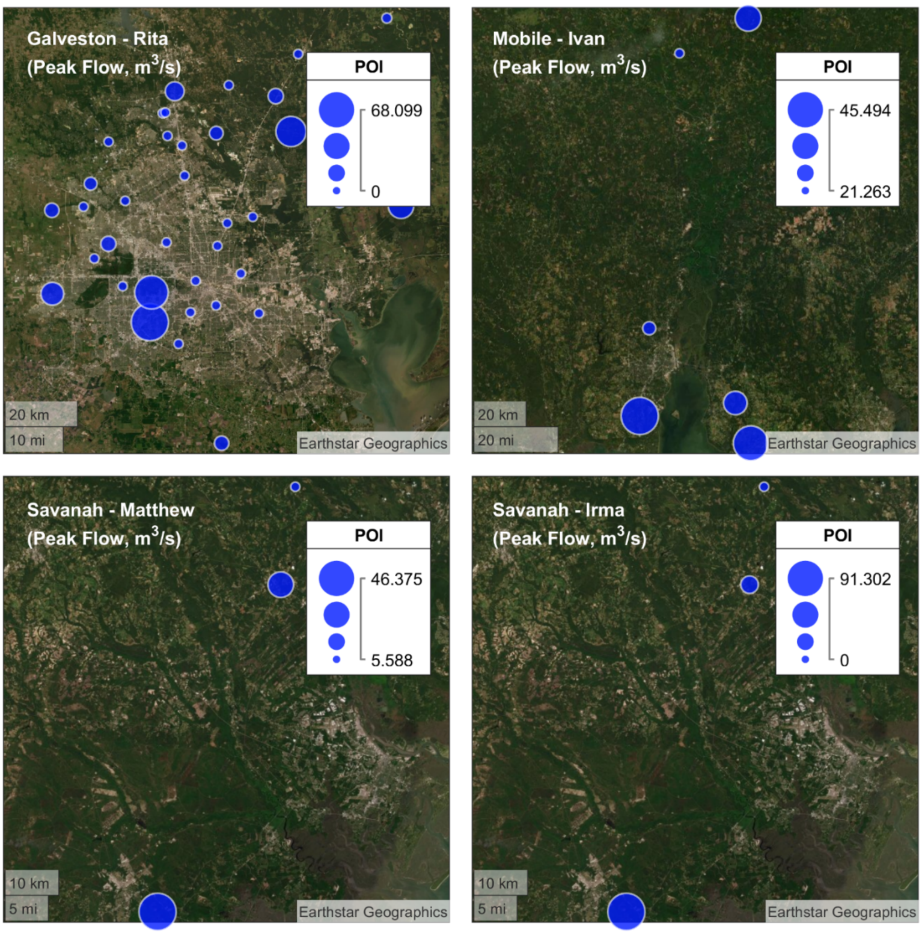

Figure 7. Streamflow forecast improved by data assimilation during peak flow conditions across the USGS stations within the Galveston, Mobile, and Savanah watersheds.

Figure 8 illustrates the ensemble streamflow forecasts with and without using data assimilation across multiple USGS stations in the Galveston watershed. As it is seen in this figure,

https://doi.org/10.5194/hess-2024-209
Preprint. Discussion started: 21 October 2024

in all locations the ensemble mean is much closer to the observation compared to the streamflow mean value from the open-loop stimulation. The shaded blue area represents the 95% uncertainty interval. We also see that in all cases the observations fall within the uncertainty interval. Therefore, we can conclude that using data assimilation, the hydrologic model results in a more accurate and precise streamflow forecasts.

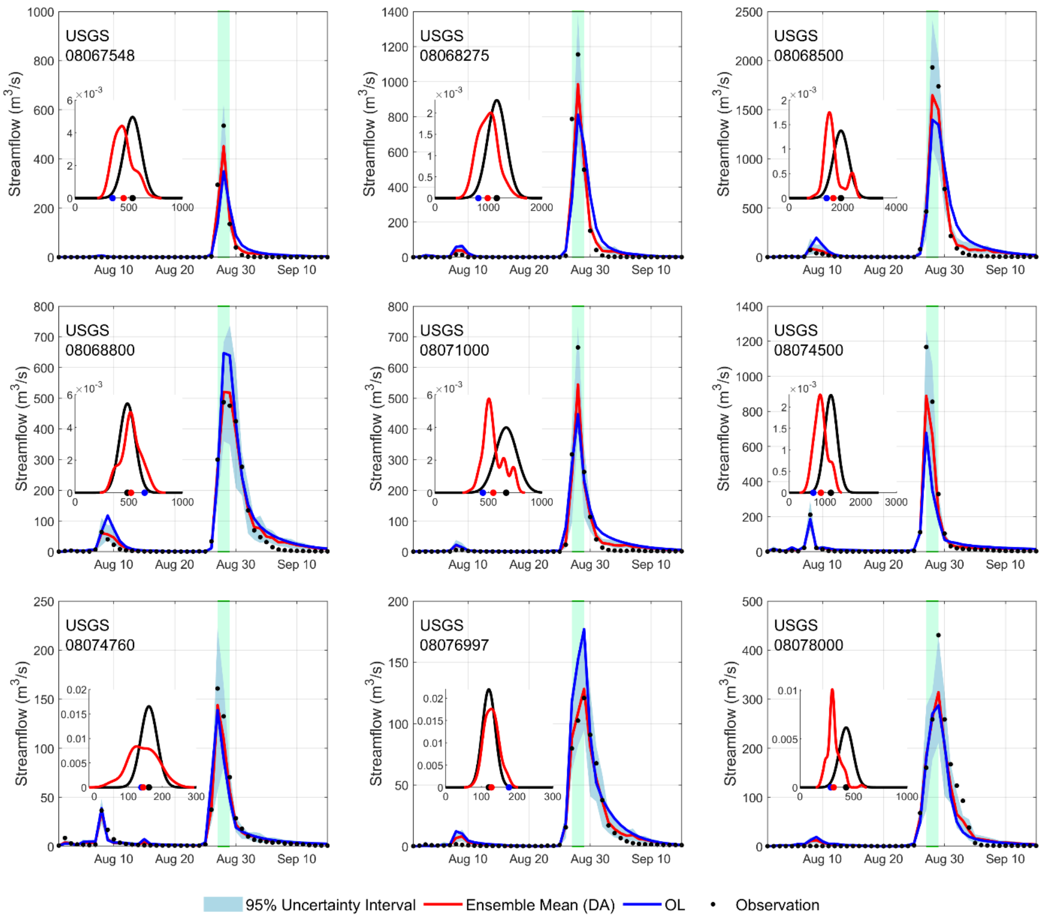

Figure 8. One-day ahead streamflow forecast with and without data assimilation across multiple USGS stations in the Galveston watershed in TX during Hurricane Harvey.

4. Conclusions

This study investigates the advantages of employing a state-of-the-art data assimilation technique, HEAVEN, to address all sources of uncertainty inherent in different layers of hydrologic simulations. It studies its impact on enhancing the SAC-SMA's forecasting capability of extreme river flow caused by hurricanes across different regions in the SEUS.

The results demonstrate that HEAVEN, with its inherent features, is a suitable approach to complement a hydrologic model, enhancing its forecasting accuracy during extreme events. Employing simultaneous operations on both batch processing and sequential modes, HEAVEN facilitates a comprehensive estimation of posterior probabilities for diverse streamflow regimes, encompassing both low and high flows. Model structural uncertainty is quantified by integrating an explicit form of the model error covariance matrix (Q) within the 4DVAR cost function. The prior error covariance matrix (B), comprising a linear combination of static (Bs) and dynamic (Bd) error covariance matrices, undergoes propagation across successive cycles throughout the assimilation period. This process effectively addresses a wide spectrum of uncertainties in model predictions, resulting in the most reliable posterior distributions. By preventing particle degeneracy and sample impoverishment, HEAVEN ensures the reliablity and accuracy of the model's outputs.

In this study, we optimized the 4DVAR cost function using the Nelder-Mead optimization algorithm since neither the tangent linear nor adjoint versions of the forecast model were available. If these were accessible, the model forecasts could have been provided much more quickly, as the current version of HEAVEN requires solving optimization problem, which is typically computationally intensive. With the current developements in hydrologic modeling utilizing Machine Learning (ML) emulators, HEAVEN is anticipated to make a significant contribution to their forecasting capabilities by effectively characterizing and accounting for uncertainty.

Competing interests

The contact author has declared that none of the authors has any competing interests.

Acknowledgment

The partial financial support for this project was provided by the USACE -ERDC contract number A20-0545-001.

Authors Contributions

P.A. wrote the first draft of the manuscript. K.G. helped with collecting and processing remote sensing products. P.A. and H.M. conceptuaized the study. H.M. edited the manuscript.

References

Abbaszadeh, P., Gavahi, K., Moradkhani, H., 2020. Multivariate remotely sensed and in-situ data assimilation for enhancing community WRF-Hydro model forecasting. Adv. Water Resour. 145, 103721. https://doi.org/10.1016/j.advwatres.2020.103721

Abbaszadeh, P., Moradkhani, H., Daescu, D.N., 2019. The Quest for Model Uncertainty Quantification: A Hybrid Ensemble and Variational Data Assimilation Framework. Water Resour. Res. 55, 2407–2431. https://doi.org/10.1029/2018WR023629

Abbaszadeh, P., Moradkhani, H., Yan, H., 2018. Enhancing hydrologic data assimilation by evolutionary Particle Filter and Markov Chain Monte Carlo. Adv. Water Resour. 111, 192–204. https://doi.org/10.1016/j.advwatres.2017.11.011

Ahmadisharaf, E., Kalyanapu, A.J., Bates, P.D., 2018. A probabilistic framework for floodplain mapping using hydrological modeling and unsteady hydraulic modeling. Hydrol. Sci. J. 63. https://doi.org/10.1080/02626667.2018.1525615

Alipour, A., Ahmadalipour, A., Abbaszadeh, P., Moradkhani, H., 2020a. Leveraging machine learning for predicting flash flood damage in the Southeast US. Environ. Res. Lett. 15, 024011. https://doi.org/10.1088/1748-9326/ab6edd

Alipour, A., Ahmadalipour, A., Moradkhani, H., 2020b. Assessing flash flood hazard and damages in the southeast United States. J. Flood Risk Manag. 13. https://doi.org/10.1111/jfr3.12605

Anderson, J.L., Anderson, S.L., 1999. A Monte Carlo Implementation of the Nonlinear Filtering Problem to Produce Ensemble Assimilations and Forecasts. Mon. Weather Rev. 127, 2741–2758. https://doi.org/10.1175/1520-0493(1999)127<2741:AMCIOT>2.0.CO;2

https://doi.org/10.5194/hess-2024-209
Preprint. Discussion started: 21 October 2024

Annis, A., Nardi, F., Volpi, E., Fiori, A., 2020. Quantifying the relative impact of hydrological and hydraulic modelling parameterizations on uncertainty of inundation maps. Hydrol. Sci. J. 65. https://doi.org/10.1080/02626667.2019.1709640

Apel, H., Thieken, A.H., Merz, B., Blöschl, G., 2004. Flood risk assessment and associated uncertainty. Nat. Hazards Earth Syst. Sci. 4. https://doi.org/10.5194/nhess-4-295-2004

Aronica, G., Bates, P.D., Horritt, M.S., 2002. Assessing the uncertainty in distributed model predictions using observed binary pattern information within GLUE. Hydrol. Process. 16. https://doi.org/10.1002/hyp.398

Bateni, S.M., Entekhabi, D., 2012. Surface heat flux estimation with the ensemble Kalman smoother: Joint estimation of state and parameters. Water Resour. Res. 48, 1–16. https://doi.org/10.1029/2011WR011542

Bates, P.D., Horritt, M.S., Aronica, G., Beven, K., 2004. Bayesian updating of flood inundation likelihoods conditioned on flood extent data. Hydrol. Process. 18. https://doi.org/10.1002/hyp.1499

Bennett, K.E., Cherry, J.E., Balk, B., Lindsey, S., 2019. Using MODIS estimates of fractional snow cover area to improve streamflow forecasts in interior Alaska. Hydrol. Earth Syst. Sci. 23. https://doi.org/10.5194/hess-23-2439-2019

Bermúdez, M., Neal, J.C., Bates, P.D., Coxon, G., Freer, J.E., Cea, L., Puertas, J., 2017. Quantifying local rainfall dynamics and uncertain boundary conditions into a nested regional-local flood modeling system. Water Resour. Res. 53. https://doi.org/10.1002/2016WR019903

Bhuyian, M.N.M., Kalyanapu, A.J., Nardi, F., 2015. Approach to Digital Elevation Model Correction by Improving Channel Conveyance. J. Hydrol. Eng. 20. https://doi.org/10.1061/(asce)he.1943-5584.0001020

Blöschl, G., Hall, J., Viglione, A., Perdigão, R.A.P., Parajka, J., Merz, B., Lun, D., Arheimer, B., Aronica, G.T., Bilibashi, A., Boháč, M., Bonacci, O., Borga, M., Čanjevac, I., Castellarin, A., Chirico, G.B., Claps, P., Frolova, N., Ganora, D., Gorbachova, L., Gül, A., Hannaford, J., Harrigan, S., Kireeva, M., Kiss, A., Kjeldsen, T.R., Kohnová, S., Koskela, J.J., Ledvinka, O., Macdonald, N., Mavrova-Guirguinova, M., Mediero, L., Merz, R., Molnar, P., Montanari, A., Murphy, C., Osuch, M., Ovcharuk, V., Radevski, I., Salinas, J.L., Sauquet, E., Šraj, M., Szolgay, J., Volpi, E., Wilson, D., Zaimi, K., Živković, N., 2019. Changing climate both increases and decreases European river floods. Nature 573. https://doi.org/10.1038/s41586-019-1495-6

Bowman, A.L., Franz, K.J., Hogue, T.S., 2017. Case studies of a MODIS-based potential evapotranspiration input to the Sacramento Soil Moisture Accounting model. J. Hydrometeorol. 18. https://doi.org/10.1175/JHM-D-16-0214.1

Bravo, J.M., Allasia, D., Paz, A.R., Collischonn, W., Tucci, C.E.M., 2012. Coupled Hydrologic-Hydraulic Modeling of the Upper Paraguay River Basin. J. Hydrol. Eng. 17. https://doi.org/10.1061/(asce)he.1943-5584.0000494

Burnash, R., Ferral, R., Richard A. McGuire, 1973. A generalized streamflow simulation system, NOAA Technical Report.

Cheng, S., Argaud, J.-P., Iooss, B., Lucor, D., Ponçot, A., 2019. Background error covariance iterative updating with invariant observation measures for data assimilation. Stoch. Environ. Res. Risk Assess. 33, 2033–2051. https://doi.org/10.1007/s00477-019-01743-6

Clark, M.P., Rupp, D.E., Woods, R.A., Zheng, X., Ibbitt, R.P., Slater, A.G., Schmidt, J., Uddstrom, M.J., 2008a. Hydrological data assimilation with the ensemble Kalman filter: Use of streamflow observations to update states in a distributed hydrological model. Adv. Water Resour. 31, 1309–1324. https://doi.org/10.1016/j.advwatres.2008.06.005

Clark, M.P., Rupp, D.E., Woods, R.A., Zheng, X., Ibbitt, R.P., Slater, A.G., Schmidt, J., Uddstrom, M.J., 2008b. Hydrological data assimilation with the ensemble Kalman filter: Use of streamflow observations to update states in a distributed hydrological model. Adv. Water Resour. 31, 1309–1324. https://doi.org/10.1016/j.advwatres.2008.06.005

Dechant, C.M., Moradkhani, H., 2012. Examining the effectiveness and robustness of sequential data assimilation methods for quantification of uncertainty in hydrologic forecasting. Water Resour. Res. 48, 1–15. https://doi.org/10.1029/2011WR011011

Dechant, C.M., Moradkhani, H., 2011. Improving the characterization of initial condition for ensemble streamflow prediction using data assimilation. Hydrol. Earth Syst. Sci. 15, 3399–3410. https://doi.org/10.5194/hess-15-3399-2011

DeChant, C.M., Moradkhani, H., 2012. Examining the effectiveness and robustness of sequential data assimilation methods for quantification of uncertainty in hydrologic forecasting. Water Resour. Res. 48. https://doi.org/10.1029/2011WR011011

Di Baldassarre, G., Montanari, A., 2009. Uncertainty in river discharge observations: A quantitative analysis. Hydrol. Earth Syst. Sci. 13. https://doi.org/10.5194/hess-13-913-2009

Dimitriadis, P., Tegos, A., Oikonomou, A., Pagana, V., Koukouvinos, A., Mamassis, N., Koutsoyiannis, D., Efstratiadis, A., 2016. Comparative evaluation of 1D and quasi-2D hydraulic models based on benchmark and real-world applications for uncertainty assessment in flood mapping. J. Hydrol. 534. https://doi.org/10.1016/j.jhydrol.2016.01.020

Domeneghetti, A., Castellarin, A., Brath, A., 2012. Assessing rating-curve uncertainty and its effects on hydraulic model calibration. Hydrol. Earth Syst. Sci. 16. https://doi.org/10.5194/hess-16-1191-2012

Domeneghetti, A., Vorogushyn, S., Castellarin, A., Merz, B., Brath, A., 2013. Probabilistic flood hazard mapping: Effects of uncertain boundary conditions. Hydrol. Earth Syst. Sci. 17. https://doi.org/10.5194/hess-17-3127-2013

Duan, Q., Sorooshian, S., Gupta, V., 1992. Effective and efficient global optimization for conceptual rainfall-runoff models. Water Resour. Res. 28, 1015–1031. https://doi.org/10.1029/91WR02985

Duan, Q.Y., Gupta, V.K., Sorooshian, S., 1993. Shuffled complex evolution approach for effective and efficient global minimization. J. Optim. Theory Appl. 76. https://doi.org/10.1007/BF00939380

https://doi.org/10.5194/hess-2024-209
Preprint. Discussion started: 21 October 2024

Hydrology and Earth System Sciences Discussions

Earth Data Science, 2021. Acquiring streamflow data from USGS with climata and Python [WWW Document]. URL https://www.earthdatascience.org/tutorials/acquire-and-visualize-usgs-hydrology-data/ (accessed 11.11.21).

Felder, G., Zischg, A., Weingartner, R., 2017. The effect of coupling hydrologic and hydrodynamic models on probable maximum flood estimation. J. Hydrol. 550. https://doi.org/10.1016/j.jhydrol.2017.04.052

Grimaldi, S., Petroselli, A., Arcangeletti, E., Nardi, F., 2013. Flood mapping in ungauged basins using fully continuous hydrologic-hydraulic modeling. J. Hydrol. 487. https://doi.org/10.1016/j.jhydrol.2013.02.023

Grimaldi, S., Schumann, G.J.P., Shokri, A., Walker, J.P., Pauwels, V.R.N., 2019. Challenges, Opportunities, and Pitfalls for Global Coupled Hydrologic-Hydraulic Modeling of Floods. Water Resour. Res. 55. https://doi.org/10.1029/2018WR024289

Hain, C.R., Crow, W.T., Anderson, M.C., Mecikalski, J.R., 2012. An ensemble Kalman filter dual assimilation of thermal infrared and microwave satellite observations of soil moisture into the Noah land surface model. Water Resour. Res. 48. https://doi.org/10.1029/2011WR011268

Jafarzadegan, K., H. Moradkhani, F. Pappenberger, H. Moftakhari, P. Bates, P. Abbaszadeh, R. Marsooli, C. Ferreira, H. Cloke, F. Ogden, and D. Qingyun (2023), Recent Advances and New Frontiers in Riverine and Coastal Flood Modeling, Reviews of Geophysics, doi:10.1007/s11625-023-01298-0

John P. Cangialosi, Andrew S. Latto, and R.B., 2017. NATIONAL HURRICANE CENTER TROPICAL CYCLONE REPORT: HURRICANE IRMA.

Koster, R.D., Liu, Q., Mahanama, S.P.P., Reichle, R.H., 2018. Improved Hydrological Simulation Using SMAP Data: Relative Impacts of Model Calibration and Data Assimilation. J. Hydrometeorol. 19, 727–741. https://doi.org/10.1175/JHM-D-17-0228.1

Kuczera, G., Parent, E., 1998. Monte Carlo assessment of parameter uncertainty in conceptual catchment models: the Metropolis algorithm. J. Hydrol. 211, 69–85. https://doi.org/10.1016/S0022-1694(98)00198-X

Laganier, O., Ayral, P.A., Salze, D., Sauvagnargues, S., 2014. A coupling of hydrologic and hydraulic models appropriate for the fast floods of the Gardon River basin (France). Nat. Hazards Earth Syst. Sci. 14. https://doi.org/10.5194/nhess-14-2899-2014

Lee, H., Seo, D.J., Koren, V., 2011. Assimilation of streamflow and in situ soil moisture data into operational distributed hydrologic models: Effects of uncertainties in the data and initial model soil moisture states. Adv. Water Resour. 34, 1597–1615. https://doi.org/10.1016/j.advwatres.2011.08.012

Lian, Y., Chan, I.C., Singh, J., Demissie, M., Knapp, V., Xie, H., 2007. Coupling of hydrologic and hydraulic models for the Illinois River Basin. J. Hydrol. 344. https://doi.org/10.1016/j.jhydrol.2007.08.004

Liberto, T. Di, 2016. Record-breaking hurricane Matthew causes devastation [WWW Document]. NOAA Clim. URL https://www.climate.gov/news-features/event-

Hydrology and Earth System Sciences Open Access EGU Discussions

tracker/record-breaking-hurricane-matthew-causes-devastation

Lievens, H., De Lannoy, G.J.M., Al Bitar, A., Drusch, M., Dumedah, G., Hendricks Franssen, H.J., Kerr, Y.H., Tomer, S.K., Martens, B., Merlin, O., Pan, M., Roundy, J.K., Vereecken, H., Walker, J.P., Wood, E.F., Verhoest, N.E.C., Pauwels, V.R.N., 2016. Assimilation of SMOS soil moisture and brightness temperature products into a land surface model. Remote Sens. Environ. 180, 292–304. https://doi.org/10.1016/j.rse.2015.10.033

Liu, C., Xiao, Q., Wang, B., 2008. An ensemble-based four-dimensional variational data assimilation scheme. Part I: Technical formulation and preliminary test. Mon. Weather Rev. 136. https://doi.org/10.1175/2008MWR2312.1

Liu, Y., Gupta, H. V., 2007. Uncertainty in hydrologic modeling: Toward an integrated data assimilation framework. Water Resour. Res. https://doi.org/10.1029/2006WR005756

Liu, Z., Merwade, V., Jafarzadegan, K., 2019. Investigating the role of model structure and surface roughness in generating flood inundation extents using one- and two-dimensional hydraulic models. J. Flood Risk Manag. 12. https://doi.org/10.1111/jfr3.12347

Mai, D.T., De Smedt, F., 2017. A combined hydrological and hydraulic model for flood prediction in Vietnam applied to the Huong river basin as a test case study. Water (Switzerland) 9. https://doi.org/10.3390/w9110879

Mallakpour, I., Villarini, G., 2015. The changing nature of flooding across the central United States. Nat. Clim. Chang. 5. https://doi.org/10.1038/nclimate2516

Marshall, L., Nott, D., Sharma, A., 2004. A comparative study of Markov chain Monte Carlo methods for conceptual rainfall-runoff modeling. Water Resour. Res. 40, 1–11. https://doi.org/10.1029/2003WR002378

Montanari, M., Hostache, R., Matgen, P., Schumann, G., Pfister, L., Hoffmann, L., 2009. Calibration and sequential updating of a coupled hydrologic-hydraulic model using remote sensing-derived water stages. Hydrol. Earth Syst. Sci. 13. https://doi.org/10.5194/hess-13-367-2009

Montzka, C., Grant, J.P., Moradkhani, H., Franssen, H.-J.H., Weihermüller, L., Drusch, M., Vereecken, H., 2013. Estimation of Radiative Transfer Parameters from L-Band Passive Microwave Brightness Temperatures Using Advanced Data Assimilation. Vadose Zo. J. 12. https://doi.org/10.2136/vzj2012.0040

Moradkhani, H., DeChant, C.M., Sorooshian, S., 2012. Evolution of ensemble data assimilation for uncertainty quantification using the particle filter-Markov chain Monte Carlo method. Water Resour. Res. 48. https://doi.org/10.1029/2012WR012144

Moradkhani, H., Hsu, K.-L., Gupta, H., Sorooshian, S., 2005. Uncertainty assessment of hydrologic model states and parameters: Sequential data assimilation using the particle filter. Water Resour. Res. 41, 1–17. https://doi.org/10.1029/2004WR003604

Moradkhani, H., Nearing, G., Abbaszadeh, P., Pathiraja, S., 2018a. Fundamentals of Data Assimilation and Theoretical Advances, in: Handbook of Hydrometeorological Ensemble Forecasting. Springer Berlin Heidelberg, pp. 1–26. https://doi.org/10.1007/978-3-642-40457-3_30-1

Moradkhani, H., Nearing, G., Abbaszadeh, P., Pathiraja, S., 2018b. Fundamentals of Data Assimilation and Theoretical Advances. Handb. Hydrometeorol. Ensemble Forecast. 1–26. https://doi.org/10.1007/978-3-642-40457-3_30-1

Mu, Q., Heinsch, F.A., Zhao, M., Running, S.W., 2007. Development of a global evapotranspiration algorithm based on MODIS and global meteorology data. Remote Sens. Environ. 111. https://doi.org/10.1016/j.rse.2007.04.015

Mu, Q., Zhao, M., Running, S.W., 2011. Improvements to a MODIS global terrestrial evapotranspiration algorithm. Remote Sens. Environ. 115. https://doi.org/10.1016/j.rse.2011.02.019

Nam, D.H., Mai, D.T., Udo, K., Mano, A., 2014. Short-term flood inundation prediction using hydrologic-hydraulic models forced with downscaled rainfall from global NWP. Hydrol. Process. 28. https://doi.org/10.1002/hyp.10084

Neal, J.C., Odoni, N.A., Trigg, M.A., Freer, J.E., Garcia-Pintado, J., Mason, D.C., Wood, M., Bates, P.D., 2015. Efficient incorporation of channel cross-section geometry uncertainty into regional and global scale flood inundation models. J. Hydrol. 529. https://doi.org/10.1016/j.jhydrol.2015.07.026

Nelder, J.A., Mead, R., 1965. A Simplex Method for Function Minimization. Comput. J. 7, 308–313. https://doi.org/10.1093/comjnl/7.4.308

Nguyen, P., Thorstensen, A., Sorooshian, S., Hsu, K., AghaKouchak, A., Sanders, B., Koren, V., Cui, Z., Smith, M., 2016. A high resolution coupled hydrologic–hydraulic model (HiResFlood-UCI) for flash flood modeling. J. Hydrol. 541. https://doi.org/10.1016/j.jhydrol.2015.10.047

Papaioannou, G., Vasiliades, L., Loukas, A., Aronica, G.T., 2017. Probabilistic flood inundation mapping at ungauged streams due to roughness coefficient uncertainty in hydraulic modelling. Adv. Geosci. 44. https://doi.org/10.5194/adgeo-44-23-2017

Pappenberger, F., Beven, K., Horritt, M., Blazkova, S., 2005. Uncertainty in the calibration of effective roughness parameters in HEC-RAS using inundation and downstream level observations. J. Hydrol. 302. https://doi.org/10.1016/j.jhydrol.2004.06.036

Pappenberger, F., Matgen, P., Beven, K.J., Henry, J.B., Pfister, L., Fraipont, P., 2006. Influence of uncertain boundary conditions and model structure on flood inundation predictions. Adv. Water Resour. 29. https://doi.org/10.1016/j.advwatres.2005.11.012

Pathiraja, S., Anghileri, D., Burlando, P., Sharma, A., Marshall, L., Moradkhani, H., 2018a. Insights on the impact of systematic model errors on data assimilation performance in changing catchments. Adv. Water Resour. 113, 202–222. https://doi.org/S030917081730670X

Pathiraja, S., Moradkhani, H., Marshall, L., Sharma, A., Geenens, G., 2018b. Data-Driven Model Uncertainty Estimation in Hydrologic Data Assimilation. Water Resour. Res. https://doi.org/10.1002/2018WR022627

Petroselli, A., Vojtek, M., Vojteková, J., 2019. Flood mapping in small ungauged basins: A comparison of different approaches for two case studies in Slovakia. Hydrol. Res. 50.

https://doi.org/10.2166/nh.2018.040

Plaza, D.A., De Keyser, R., De Lannoy, G.J.M., Giustarini, L., Matgen, P., Pauwels, V.R.N., 2012. The importance of parameter resampling for soil moisture data assimilation into hydrologic models using the particle filter. Hydrol. Earth Syst. Sci. 16, 375–390. https://doi.org/10.5194/hess-16-375-2012

Richard D. Knabb, Daniel P. Brown, and J.R.R., 2006. Tropical Cyclone Report Hurricane Rita.

Ryan McNeill and Duff Wilson, 2017. Exclusive: At least $23 billion of property affected by Hurricane Harvey - Reuters analysis [WWW Document]. Reuters. URL https://www.reuters.com/article/us-storm-harvey-property-exclusive/exclusive-at-least-23-billion-of-property-affected-by-hurricane-harvey-reuters-analysis-idUSKCN1BA31P

Samuel, J., Coulibaly, P., Metcalfe, R.A., 2011. Estimation of Continuous Streamflow in Ontario Ungauged Basins: Comparison of Regionalization Methods. J. Hydrol. Eng. 16. https://doi.org/10.1061/(asce)he.1943-5584.0000338

Savant, G., Berger, C., McAlpin, T.O., Tate, J.N., 2011. Efficient Implicit Finite-Element Hydrodynamic Model for Dam and Levee Breach. J. Hydraul. Eng. 137. https://doi.org/10.1061/(asce)hy.1943-7900.0000372

Savant, G., Berger, R.C., 2012. Adaptive Time Stepping–Operator Splitting Strategy to Couple Implicit Numerical Hydrodynamic and Water Quality Codes. J. Environ. Eng. 138. https://doi.org/10.1061/(asce)ee.1943-7870.0000547

Scharffenberg, W.A., Kavvas, M.L., 2011. Uncertainty in Flood Wave Routing in a Lateral-Inflow-Dominated Stream. J. Hydrol. Eng. 16. https://doi.org/10.1061/(asce)he.1943-5584.0000298

Shaw, J.A., Daescu, D.N., 2016. An ensemble approach to weak-constraint four-dimensional variational data assimilation. Procedia Comput. Sci. 80, 496–506. https://doi.org/10.1016/j.procs.2016.05.329

Sindhu, K., Durga Rao, K.H.V., 2017. Hydrological and hydrodynamic modeling for flood damage mitigation in Brahmani–Baitarani River Basin, India. Geocarto Int. 32. https://doi.org/10.1080/10106049.2016.1178818

Smith, M.B., Laurine, D.P., Koren, V.I., Reed, S.M., Zhang, Z., 2003. Hydrologic Model calibration in the National Weather Service. pp. 133–152. https://doi.org/10.1029/WS006p0133

Stewart, S.R., 2017. National Hurricane Center Tropical Cyclone Report: Hurricane Matthew. Natl. Hurric. Cent. Trop. Cyclone Rep. 5.

The Seattle Times, 2021. Harvey recovery continues in parts of flooded Liberty County [WWW Document]. URL https://www.seattletimes.com/nation-world/harvey-recovery-continues-in-parts-of-flooded-liberty-county/ (accessed 11.11.21).

Thomas Steven Savage, J., Pianosi, F., Bates, P., Freer, J., Wagener, T., 2016. Quantifying the importance of spatial resolution and other factors through global sensitivity analysis of a flood inundation model. Water Resour. Res. 52. https://doi.org/10.1002/2015WR018198

https://doi.org/10.5194/hess-2024-209
Preprint. Discussion started: 21 October 2024

Hydrology and Earth System Sciences Discussions
Open Access
EGU

TPWD [WWW Document], 2021. URL https://tpwd.texas.gov/newsmedia/releases/?req=20050927a (accessed 11.11.21).

Tripathy, S., K. Jafarzadegan, H. Moftakhari, and H. Moradkhani (2024), Dynamic Bivariate Hazard Forecasting of Hurricanes for Improved Disaster Preparedness, Communications Earth & Environment, doi:10.1038/s43247-023-01198-2

Trémolet, Y., 2007. Model-error estimation in 4D-Var. Q. J. R. Meteorol. Soc. 133, 1267–1280. https://doi.org/10.1002/qj.94

USGS, 2021a. USGS [WWW Document]. URL https://waterdata.usgs.gov/nwis/dv/?ts_id=133980,173616,173617&format=img_default&site_no=08066500&begin_date=20170817&end_date=20170906 (accessed 11.11.21).

USGS, 2021b. USGS [WWW Document]. URL https://waterdata.usgs.gov/nwis/dv/?ts_id=133980,173616,173617&format=img_default&site_no=08066500&begin_date=20050918&end_date=20050930 (accessed 11.11.21).

USGS [WWW Document], 2021c. URL https://waterdata.usgs.gov/usa/nwis/uv?site_no=02428400 (accessed 11.11.21).

Vacondio, R., Dal Palù, A., Mignosa, P., 2014. GPU-enhanced finite volume shallow water solver for fast flood simulations. Environ. Model. Softw. 57. https://doi.org/10.1016/j.envsoft.2014.02.003

Vrugt, J.A., Gupta, H. V., Nualláin, B.Ó., Bouten, W., 2006. Real-time data assimilation for operational ensemble streamflow forecasting. J. Hydrometeorol. 7, 548–565. https://doi.org/10.1175/JHM504.1

Wahlstrom, M., Guha-Sapir, D., 2015. The human cost of weather-related disasters 1995-2015, UNISDR Publications.

Werner, M., Blazkova, S., Petr, J., 2005. Spatially distributed observations in constraining inundation modelling uncertainties. Hydrol. Process. 19. https://doi.org/10.1002/hyp.5833

Xia, Y., Mitchell, K., Ek, M., Sheffield, J., Cosgrove, B., Wood, E., Luo, L., Alonge, C., Wei, H., Meng, J., Livneh, B., Lettenmaier, D., Koren, V., Duan, Q., Mo, K., Fan, Y., Mocko, D., 2012. Continental-scale water and energy flux analysis and validation for the North American Land Data Assimilation System project phase 2 (NLDAS-2): 1. Intercomparison and application of model products. J. Geophys. Res. 117, 1–27. https://doi.org/10.1029/2011JD016048

Yan, H., DeChant, C.M., Moradkhani, H., 2015. Improving Soil Moisture Profile Prediction With the Particle Filter-Markov Chain Monte Carlo Method. IEEE Trans. Geosci. Remote Sens. 53, 6134–6147. https://doi.org/10.1109/TGRS.2015.2432067

Yan, H., Moradkhani, H., 2016. Combined assimilation of streamflow and satellite soil moisture with the particle filter and geostatistical modeling. Adv. Water Resour. 94, 364–378. https://doi.org/10.1016/j.advwatres.2016.06.002

Zischg, A.P., Felder, G., Mosimann, M., Röthlisberger, V., Weingartner, R., 2018. Extending coupled hydrological-hydraulic model chains with a surrogate model for the estimation of

https://doi.org/10.5194/hess-2024-209
Preprint. Discussion started: 21 October 2024

Hydrology and Earth System Sciences
Discussions

flood losses. Environ. Model. Softw. 108. https://doi.org/10.1016/j.envsoft.2018.08.009